پنجمین کنفرانس منطقه‌ای سیرد
5th REGIONAL CONFERENCE ON
ELECTRICITY DISTRIBUTION
Tehran - Jan. 2017

Simulating and Comparing the Transient Behavior of Different Models of MV Metal Oxide Surge Arresters

Mahmoud Eshagh Ahmadi, Mohsen Niasati, Mohammad Reza Barzegar-Bafruee
Faculty of Electrical and Computer Engineering
Semnan University
Semnan, Iran
M.ahmadi@semnan.ac.ir

Abstract_The results of measuring residual voltage of metal oxide surge arresters (MOSAs) show that MOSA has dynamic behavior against switching and lightning overvoltages. For this reason, to obtain the real behavior of MOSA, several models have been proposed. In this paper, regarding the importance of MOSA modeling and selecting an appropriate model in different studies, four models-IEEE, Pinceti, Fernandez, and P-K are analyzed under different scenarios. The simulation results are also compared with the manufacturer's data and the accuracy of mentioned models are determined in details. This study, which is performed by EMTP-RV® software, indicates that concentrating on the particular model for all studies does not provide the appropriate accuracy.

Keywords: Metal oxide surge arrester, Arrester models, Lightning, Switching, Transient overvoltages.

1- Introduction

Power system equipment are vulnerable against transient overvoltages which are characterized by the extreme high amplitude and frequency. Therefore, it is essential the protection of the power system equipment against these waves. As one of the promising approaches, metal oxide surge arrester (MOSA) has been introduced to protect electrical equipment against transient overvoltages and current discharging [1–2]. Surge arresters (SAs) that operate as same as the voltage limiter, transfer stored energy in transient waves into the ground. Such operation prevents from dielectric breakdown and increases reliability.

There are different types of SAs; however, due to the excellent non-linear V-I characteristic, MOSA has been preferred with other ones (like silicon carbide). MOSA that is formed from the series or parallel non-linear resistance, provides the astounding nonlinear V-I characteristic. In operating voltage, it has very high resistance and little loss. However, at lightening or switching over voltages, its resistance reduces quickly. In medium voltage type, to prevent leakage current, manufacturers add air gap in the structure of MOSA. The modern high voltage types are also constructed from metal oxide disks in porcelain or polymer housing [1-2].

Neglecting the advantages of applying MOSA in power system, computer simulation is a very valuable tool in many different contexts. It makes it possible to investigate a multitude of different structural properties in the design and construction phase, as well as the expected general behavior and performance in the application phase. Therefore, computer simulations are really a cost-effective method. However, the quality of computer simulations can only be as good as the quality of the built-in models and the applied data. In particular, MOSA has a nonlinear nature, and even temperature can also affect its performance [3]. The modeling of linear systems is generally so much easier than the non-linear systems and the results have lower error, Therefore, the modeling of actual transient behavior of MOSA is not easy. Attempts to identify the non-linear characteristic of MOSA and numerous application of MOSA in power system have been caused the presentation of various frequency-dependent models for simulating MOSA [4–10]. In among of the proposed models, IEEE, Pinceti, Fernandez, and P-K models are more common and have shown acceptable accuracy in different studies. In this paper, due to necessity, the performance of mentioned models is comprehensively evaluated under different transient waves.

In this paper, regarding the importance of these four models, the parameters of each model and required data are extensively described. Then, referring to the a few previous studies in term of comparison of MOSA models [5], [11–12], the transient behavior of mentioned models are analyzed under standard switching and lightning transient waves with the help of EMTP-RV® software. Finally, considering manufacturer's data, the accuracy of mentioned models is evaluated in details.

2- The Proposed Models for MOSA

MOSA is made of nonlinear resistors stacks in a one or more column. The common material used in this surge arresters, are mainly made of Zinc. For this reason, MOSAs are also known as Zinc Oxide (ZnO) surge arresters. The main characteristic of MOSA is an extreme non-linear V-I curve with high energy absorption; however, the frequency and temperature can affect the metal oxide substances. Temperature dependence appears in low current (less than 10A) and it can be neglected in transient overvoltages studies. But, the frequency-dependent of the metal oxide substances can impact on wave front-time and residual voltage of MOSA. Experimental results indicate that at the same condition for discharge current amplitude, as the crest time of the current wave decreases from 8μs to 1.3μs, the residual voltage approximately increases about 6% [7]. According to the above description, MOSAs cannot be modelled as a nonlinear resistor. Therefore, different frequency-dependent models to simulate actual transient behavior of MOSA has been proposed. In this paper, four prominent MOSA models (IEEE, Pinceti, Fernandez, and P-K) are analyzed in details.

2-1- IEEE model

This model presented in [7] is shown in Fig. 1. In IEEE model, A_0 and A_1 are two non-linear resistors that are separated by an RL filter. The values of A_0 and A_1 are given in Table 1. In discharge currents with high rise time, the effect of RL filter can be neglected. In this case, the two parallel non-linear resistors impact on the static behavior of MOSA. In the case of short front-time, filter impedance is large and, thereby, L_1 leads high currents to the A_0 resistor branch.

In the model, L_0 represents the inductance associated with magnetic fields in the immediate vicinity of the arrester. The resistor R_0 is also used to stabilize the numerical integration when the model is implemented in a digital computer program. The capacitance C_0 represents the external capacitance that is proportional to the height of MOSA.

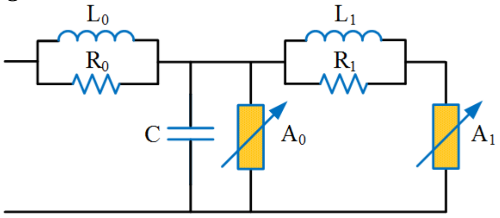

Fig. 1. IEEE model of MOSA [7].

In related to this model, the above-mentioned parameters are calculated as follows:

$$
\begin{aligned}
&\mathrm{L}_0 = 0.2d/n \ (\mu\mathrm{H}) \\
&\mathrm{R}_0 = 100d/n \ (\Omega) \\
&\mathrm{L}_1 = 15d/n \ (\mu\mathrm{H}) \\
&\mathrm{R}_1 = 65d/n \ (\Omega) \\
&\mathrm{C} = 100n/d \ (\mathrm{pF})
\end{aligned} \tag{1}
$$

Where d is the estimated height of the arrester in meter (obtained from manufacturer’s data) and n is the number of parallel columns of metal oxide in the arrester. The parameter L_1 has the most influence on the results; however, equation related to L_1 computes the initial value and does not acceptable accuracy. Hence, to increase the accuracy of the model, L_1 should be adjusted by trial and error procedure to match the residual voltages for lightning discharge currents published in the manufacturer's catalog [13]. Trial and error process and the need for the physical dimensions of arrester are significant restrictions of IEEE model. Therefore, to overcome the restrictions, various based on this structure models have been suggested in recent years. In this paper, the three popular structures that are derived from the IEEE model are comprehensively analyzed.

Table 1. V-I characteristic for A_0 and A_1.

I (A)	A_0 V (pu)	A_1 V (pu)
10	0.857	0
100	0.936	0.769
1000	1.05	0.85
2000	1.088	0.894
4000	1.125	0.925
6000	1.138	0.938
8000	1.169	0.956
10000	1.188	0.969
12000	1.206	0.975
14000	1.231	0.988
16000	1.25	0.994
18000	1.281	1
2000	1.313	1.006

2-2- Pinceti model

Fig. 2 shows the schematic of this model [8]. The model has been derived from the IEEE model with minor changes. The definition of non-linear resistors characteristics (A_0 and A_1) is completely coincided with previous subsection. The proposed criteria does not take into consideration any physical characteristic of the arrester and just electrical data are needed. The flowchart of Fig. 3 shows the process of computing L_0 and L_1. Where V_n, V_{r1}/T_2 and $V_{r8/20}$ are the rated voltage of arrester, residual voltage at 10 kA fast front current surge (l/T_2 µs), and residual voltage at 10 kA current surge with a 8/20µs shape, respectively. The decrease time (T_2) is not explicitly written because different manufacturers may use different values. R_1 is considered to avoid numerical troubles and its value is 1MΩ.

2-3- Fernandez model

The proposed model is the another simplified model of IEEE [9]. As shown in Fig. 4, two constant resistors (R_0 and R_1) and one inductance (L_0) are eliminated from IEEE model. To determine the inductance (L_1) and capacitance (C_1) of the model, equations (2) and (3) are applicable. Where V_{ss} (kV) is the residual voltage at 500A and switching wave 60µs/200µs or 30µs /70µs. Finally, the value of R is considered 1MΩ for numerical oscillations in a digital computer program. In the same way, the computation of capacitance in Fernandez model is exactly identical to IEEE model.

$$L_1 = \frac{2}{5} \cdot \frac{V_{r8/20} - V_{ss}}{V_{r8/20}} . V_n \ (\mu H) \tag{2}$$

$$C = \frac{100}{d} \ (pF) \tag{3}$$

2-4- P-K model

Fig. 5 shows the structure of the P-K model [10]. Similar Fernandez model, it is just defined L_1 where is determined form equation (4). As well as, the value of parallel resistance is assumed 1MΩ for the analytical and simulation studies. In order to simulate the dynamic characteristic of mentioned model, It is performed by discharge currents with front times starting from 0.5µs to 8µs.

$$L_1 = \frac{9}{10} \cdot \frac{V_{r1/T_2} - V_{r8/20}}{V_{r8/20}} . V_n \ (\mu H) \tag{4}$$

3- Simulation results

In this section, transient behavior of mentioned models is investigated using lightning (8/20 µs) and switching (30/60 µs) surges. The double exponential waveform is used in the simulation studies. In order to evaluate the accuracy of the models, the obtained results from the simulations are compared with the data provided in the manufacturer's catalog. As well as, to validate the obtained results and universalize the topic, three MOSAs are evaluated at medium voltage level. Table 2 gives the MOSAs' information extracted from the manufacturer's catalog [14]. Referring to previous section and Table 2, it can be obtained the parameters of mentioned models. Table 3 describes the value of parameters for each arrester.

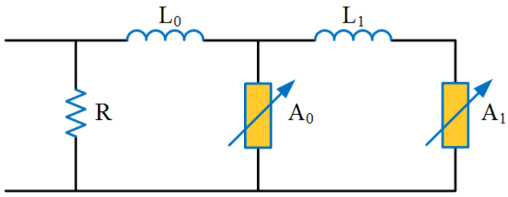

Fig. 2. Pinceti model of MOSA [8].

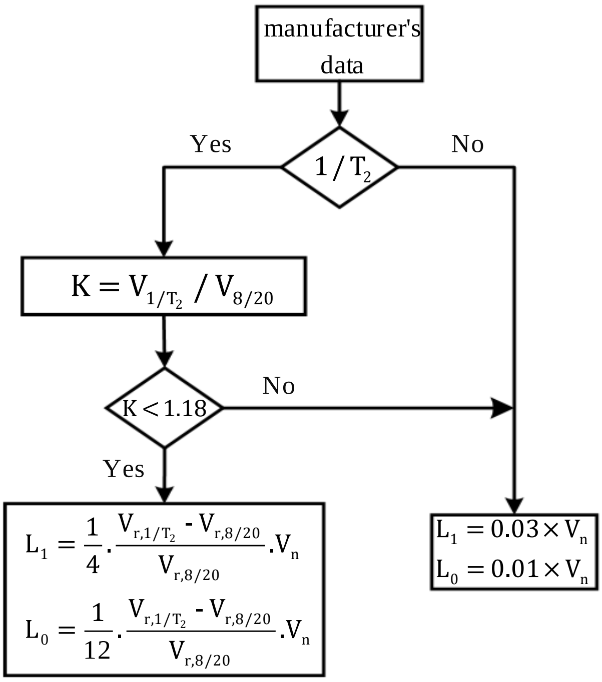

Fig. 3. The process of computing L_0 and L_1.

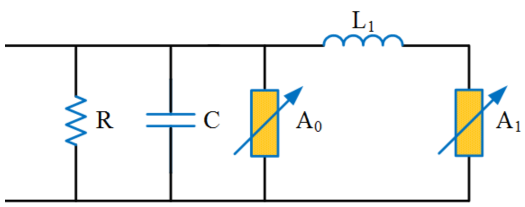

Fig. 4. Fernandez model of MOSA [9].

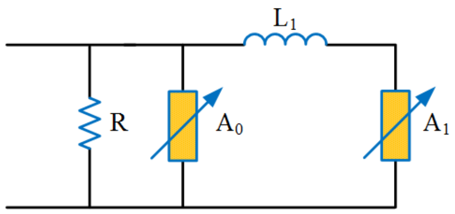

Fig. 5. P-K model of MOSA [10].

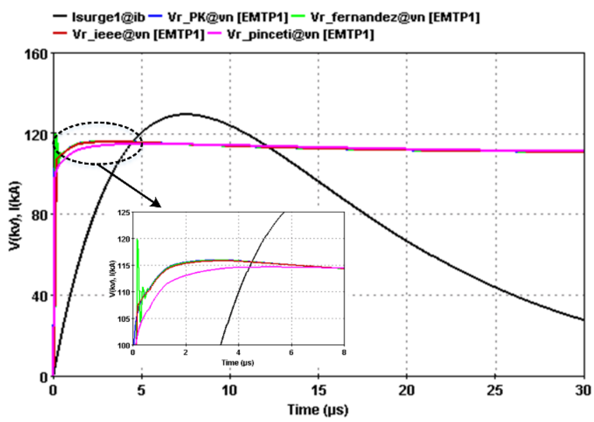

Fig. 6. Residual voltages for 5kA(8/20)µs wave (the scale of current curve is 26).

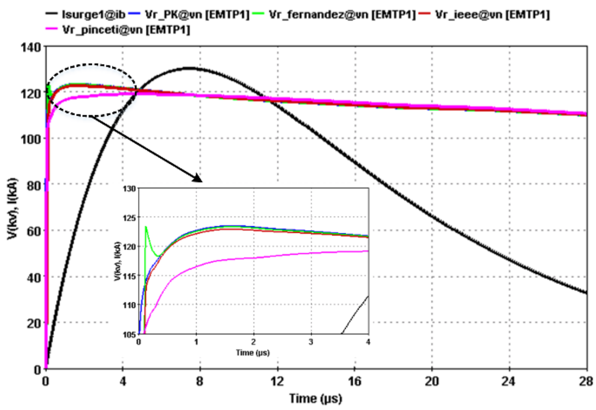

Fig. 7. Residual voltages for 10kA(8/20)µs wave (the scale of current curve is 13).

Table 2. Manufacturer's data [14].

U_r(kV)	V_{res}(kV)			
	30/60(µs)		8/20(µs)	
	0.25kA	0.5kA	5kA	10kA
10	19	19.7	23.3	24.6
30	56.7	59	69.6	73.7
50	94.6	98.3	116	122.8

By applying lightning wave with 5kA and 10kA amplitude and 8/20 µs characteristic to the different models of MOSA, the residual voltage of 50kV MOSA brings the curves like Figs. 7 and 8 for different models. It can be observed that Pinceti model indicates less residual voltage in both cases; so that the maximum residual voltage for 5kA and 10kA lightning surges are equal to 114.571kA and 119.131kV, respectively. By comparing these values with real data derived from the manufacturer's catalog, the significant error in pinceti model is observed. It can be used the following equation to calculate the amount of the error:

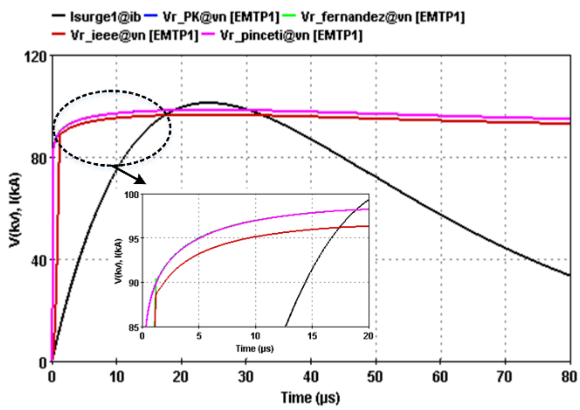

Fig. 8. Residual voltages for 0.25kA(30/60)µs wave (current curve scaled 410 times).

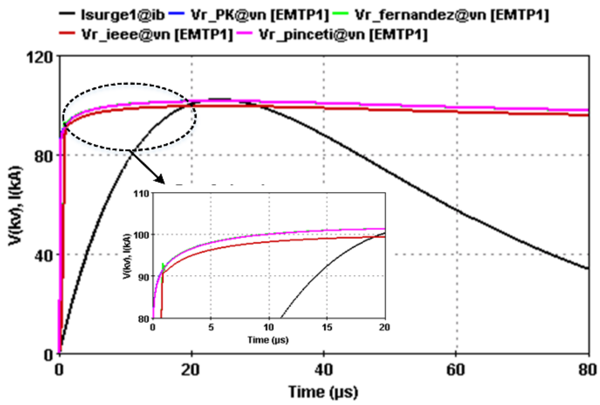

Fig. 9. Residual voltages for 0.5kA(30/60)µs wave (the scale of current curve is 205).

$$Err. = \frac{V_{res(Sim)} - V_{res(Man)}}{V_{res(Man)}} \times 100 \qquad (5)$$

Where $V_{res(Sim)}$ and $V_{res(Man)}$ are the obtained residual voltages from simulation and manufacturer's data, respectively.

Table 4 gives the maximum residual voltage and error percentage of each model when the lightning wave is applied to presented MOSAs in Table 2. As a result, Fernandez model and the P-K model introduce the maximum and minimum errors, respectively. In the case of applying 10kA lightning current to models, IEEE model gives minimum error compared with other models. The reason for the reduction of IEEE error is related to L_1. Because this parameter is obtained from trial and error process.

As switching waves 0.25kA(60/30)µs and 0.5kA(60/30)µs are applied to different models of MOSA, residual voltage of 50kV MOSA experiences the curves shown in Figs. 8 and 9. In this case, all the models have the same peak value except IEEE model. The behavior of all the models depends on the wave shape and front-time of applied wave. Moreover, in lightning wave a recursive mode occurs in the Fernandez model, whereas it do not happen in switching wave.

The error value of each model for switching wave is expressed in table 5. As a result, by comparing error values of lightning wave with switching ones, it can be found out that all of the models have the less errors for lightning wave, which reflects the better performance of the models for the lightning wave. The results also indicate that the models of MOSA depend on frequency. Indeed, the proposed models have been optimized for lightning waves.

In related to the impact of rated voltage of MOSA on the error value of the models, it can be observed the significant effect. Except Fernandez model, in other models the error value of lightning wave approximately decreases as the rated of MOSA increases (given in Tables 4 and 5). In switching wave case, the error value increases when the arrester rated voltage increases.

In addition, the residual voltage of arrester, absorption energy related to each model is also dedicated in Tables 4 and 5. In all of the models, absorbed energy is equal. Because the A_0 resistance in all of the models is equal.

4- Conclusion

In this paper, four common metal oxide surge arrester models, IEEE, Pinceti, Fernandez, and P-K were comprehensively analyzed and compared in different scenarios. The components of mentioned models and their value were fully expressed. Then, the error of each model is calculated under lightning and switching waves for three-surge arrester selected from manufacturer's catalog. As a result, the behavior of all the models depends on the wave shape and front-time of applied wave. In general, all of the models have the less errors for lightning wave, which reflects the better performance of the models for this wave. In terms of the amount of error, P-K and IEEE models also showed the less error in comparison of Pinceti and Fernandez models.

References

[1] V. Hinrichsen, "Metal-oxide surge arrester," Siemens AG, 2012.

[2] IEEE Std C62.22a, IEEE Guide for the Application of Metal-Oxide Surge Arresters for Alternating-Current Systems—Amendment 1: Supplement to Consider Energy Handling Capabilities, vol. 2013, no. July. 2013.

[3] J. A. Martinez and D. W. Durbak, "Parameter determination for modeling systems transients-Part V: Surge arresters," IEEE Trans. Power Deliv., vol. 20, no. 3, pp. 2073–2078, 2005.

[4] K. Mardira and T. Saha, "A simplified lightning model for metal oxide surge arrester," Australas. Univ. Power …, pp. 4–9, 2002.

[5] A. Bayadi, N. Harid, K. Zehar, and S. Belkhiat, "Simulation of metal oxide surge arrester dynamic behavior under fast transients," in The international Conference on Power Systems Transients (IPST'03) in New Orleans, USA, 2003.

[6] I. Kim, T. Funabashi, H. Sasaki, T. Hagiwara, and M. Kobayashi, "Study of ZnO arrester model for steep front wave," IEEE Trans. power Deliv., vol. 11, no. 2, pp. 834–841, 1996.

[7] R. A. Jones, P. R. Clifton, G. Grotz, M. Lat, F. Lembo, D. J. Melvold, D. Nigol, J. P. Skivtas, A. Sweetana, and D. F. Goodwin, "MODELING OF METAL-OXIDE SURGE ARRESTERS," IEEE Trans. Power Deliv., vol. 7, no. 1, pp. 302–309, 1992.

[8] P. Pinceti and M. Giannettoni, "A simplified model for zinc oxide surge arresters," IEEE Trans. Power Deliv., vol. 14, no. 2, pp. 393–398, Apr. 1999.

[9] F. Fernandez and R. Diaz, "Metal oxide surge arrester model for fast transient simulations," in The Int. Conf. on Power System Transients IPAT, 2001, vol. 1.

[10] P. Unahalekhaka, "Simplified Modeling of Metal Oxide Surge Arresters," Energy Procedia, vol. 56, pp. 92–101, 2014.

[11] G. V. N. Bezerra, L. A. M. M. Nobrega, J. F. S. Junior, G. R. S. Lira, V. S. Brito, E. G. Costa, and M. J. A. Maia, "Evaluation of surge arrester models for overvoltage studies," in 2014 ICHVE International Conference on High Voltage Engineering and Application, 2014, pp. 1–4.

[12] A. Meister, R. A. Shayani, and M. G. A. de Oliveira, "Comparison of metal oxide surge arrester models in overvoltage studies," Int. J. Eng. Sci. Technol., vol. 3, no. 11, pp. 35–45, 2011.

[13] M. Nafar, G. B. Gharehpetian, and T. Niknam, "A new parameter estimation algorithm for metal oxide surge arrester," Electr. Power Components Syst., vol. 39, no. 7, pp. 696–712, 2011.

[14] A. B. B. M. W. K. S. A. Datasheet, "Medium Voltage Products & Systems. Catalog 2013." 2013.

Table 3. Calculated parameters of different MOSA models

Parameter	۱m, n=۰/۱۸۷kV, d=۱۰Un=				۱m, n=۰/۳٤۷kV, d=۳۰Un=				Un=۵۰kV, d=۰/۵۰۷m, n=۱			
	IEEE	Pinceti	Fernandez	P-K	IEEE	Pinceti	Fernandez	P-K	IEEE	Pinceti	Fernandez	P-K
$L_0(\mu H)$	۰/۰۳۷٤	۰/۰۷۸۸	-	-	۰/۰٦۹٤	۰/۲۲۷	-	-	۰/۱۰۱٤	۰/۳۷٦	-	-
$L_1(\mu H)$	۲/۸۰٥	۰/۲۳۳	۰/۷۹٦	۰/۸٤۱	٥/۲۰٥	۰/٦۸۱۸	۲/۳۹۳	۲/٤٥٤	۷/٦۰٥	۱/۱۲۹	۳/۹۹	٤/۰٦۷
$L^*_1(\mu H)$	۰/۷۱	-	-	-	۲/۱٥	-	-	-	۳/٦	-	-	-
$R_0(\Omega)$	۱۸/۷	-	-	-	۳٤/۷	-	-	-	٥۰/۷	-	-	-
$R_1(\Omega)$	۱۲/۱٥٥	-	-	-	۲۲/٥٥	-	-	-	۳۲/۹٥٥	-	-	-
$C(pF)$	٥۳٤/۷٥	-	۵۳۴/۷۵	-	۲۸۸/۱۸	-	۲۸۸/۱۸	-	۱۹۷/۲۳	-	۱۹۷/۲۳	-

Table 4. Simulation results for different MOSA models as lightning wave is applied to MOSA (residual voltage (kV) and absorbed energy (kJ))

Arrester model	kV١٠Ur=				kV٣٠Ur=				kV٥٠Ur=			
	۵kA(٨/٢٠)μs		١٠kA(٨/٢٠)μs		۵kA(٨/٢٠)μs		١٠kA(٨/٢٠)μs		۵kA(٨/٢٠)μs		١٠kA(٨/٢٠)μs	
	V_{res}	E	V_{res}	E	V_{res}	E	V_{res}	E	V_{res}	E	V_{res}	E
IEEE	/١٨٢٥ ٢٣	/٣٤٩ ٢	/٦٠٥٥ ٢٤	/٧٩١ ٤	٦٩/٤٦٠	/٠٣٨ ٧	/٧٠٨٤ ٧٣	/٣٥٥ ١٤	/٧٤٩٥ ١١٥	/٧٢٨ ١١	/٨٤٥٨ ١٢٢	/٩٢٠ ٢٣
%Err.	-٠/٥	-	٠/٠٢	-	-٠/٢	-	٠/٠١	-	-٠/٢١	-	٠/٠٣٧	-
Pinceti	٢٢/٩٥٦	/٣٤٩ ٢	/٨٧١٦ ٢٣	/٧٨٩ ٤	/٧٦٨٦ ٦٨	/٠٣٨ ٧	/٥٠١٨ ٧١	/٣٤٩ ١٤	١١٤/٥٨١	/٧٢٨ ١١	/١٣١٥ ١١٩	/٩٠٩ ٢٣
%Err.	-١/٤٧	-	-٢/٩٦	-	-١/١٩	-	-٢/٩	-	-١/٢٢	-	-٢/٩	-
Fernandez	/٧٤٢٦ ٢٣	/٣٤٩ ٢	/٦٨٧٧ ٢٤	/٧٩٠ ٤	/٧٨١٨ ٧١	/٠٣٨ ٧	٧٣/٩٧٦	/٣٥١ ١٤	/٨٩٥١ ١١٩	/٧٢٨ ١١	/٣٦٨٨ ١٢٣	/٩١٢ ٢٣
%Err.	١/٨٩	-	٠/٣٥	-	٣/١٣	-	٠/٣٧	-	٣/٣٥	-	٠/٤٦	-
P-K	/٢٣٢٣ ٢٣	/٣٤٩ ٢	/٧٨٣٣ ٢٤	/٧٩٠ ٤	/٥٥٨٢ ٦٩	/٠٣٨ ٧	/١٠٧١ ٧٤	/٣٥١ ١٤	/٨٨٤٦ ١١٥	/٧٢٨ ١١	/٤٣١٤ ١٢٣	/٩١٣ ٢٣
%Err.	-٠/٢٩	-	٠/٧٤	-	-٠/٠٦	-	٠/٥٥	-	-٠/١	-	٠/٥١	-

Table 5. Simulation results for different arrester models b as switching wave is applied to MOSA (residual voltage (kV) and absorbed energy (kJ))

Arrester model	kV١٠Ur=				kV٣٠Ur=				kV٥٠Ur=			
	/٢۵kA(٣٠/۶٠)μs ٠		/۵kA(٣٠/۶٠)μs ٠		/٢۵kA(٣٠/۶٠)μs ٠		/۵kA(٣٠/۶٠)μs ٠		٠/٢۵k(٣٠/۶٠)μs		٠/۵kA(٣٠/۶٠)μs	
	V_{res}	E	V_{res}	E	V_{res}	E	V_{res}	E	V_{res}	E	V_{res}	E
IEEE	١٩/٢٥٢	٠/٣٠٧	١٩/٨٤٨	/٦٣٩ ٠	٥٧/٧٩٥	٠/٩٢٢	/٥٩٠٦ ٥٩	/٩٢١ ١	/٣٧٩٥ ٩٦	/٥٣٨ ١	٩٩/٣٧١٧	/٢٠٣ ٣
%Err.	١/٣٢	-	٠/٧٥	-	١/٧٥	-	١	-	١/٨٨	-	١/٠٩	-
Pinceti	١٩/٦٩١٨	٣١۴	/٣٠٢٧ ٢٠	٦٥٤	٥٨/٩٩٩٥	٠/٩٤٢	/٨٢٥٣ ٦٠	/٩٦١ ١	/٢٩٧٦ ٩٨	/٥٧٠ ١	/٣٤٧٧ ١٠١	/٢٦٨ ٣
%Err.	٣/٦٤	-	٣/٠٥	-	٢/١١	-	٣/٠٩	-	٣/٨٨	-	٣/١	-
Fernandez	١٩/٦٩١٨	٠/٣١۴	/٣٠٢٨ ٢٠	/٦٥٤ ٠	٥٨/٩٩٩٥	٠/٩٤٢	/٨٢٥٦ ٦٠	/٩٦١ ١	/٢٩٧٧ ٩٨	/٥٧٠ ١	/٣٤٨٢ ١٠١	/٢٦٨ ٣
%Err.	٣/٦٤	-	٣/٠٥	-	٢/١١	-	٣/٠٩	-	٣/٨٨	-	٣/١	-
P-K	١٩/٦٩١٨	٠/٣١۴	/٣٠٢٨ ٢٠	/٦٥٤ ٠	٥٨/٩٩٩٥	٠/٩٤٢	/٨٢٥٧ ٦٠	/٩٦١ ١	/٢٩٧٨ ٩٨	/٥٧٠ ١	/٣٤٨٣ ١٠١	/٢٦٨ ٢
%Err.	٣/٦٤	-	٣/٠٥	-	٢/١١	-	٣/٠٩	-	٣/٨٨	-	٣/١	-